Available online at www.sciencedirect.com

SCIENCE DIRECT®

Toxicology and Applied Pharmacology 205 (2005) 188–200

Toxicology and Applied Pharmacology

www.elsevier.com/locate/ytaap

Alteration at translational but not transcriptional level of transferrin receptor expression following manganese exposure at the blood–CSF barrier in vitro

G. Jane Li, Qiuqu Zhao, Wei Zheng*

School of Health Sciences, Purdue University, 550 Stadium Mall Drive, Room 1163D, West Lafayette, IN 47907, USA

Received 24 June 2004; accepted 6 October 2004

Abstract

Manganese exposure alters iron homeostasis in blood and cerebrospinal fluid (CSF), possibly by acting on iron transport mechanisms localized at the blood–brain barrier and/or blood–CSF barrier. This study was designed to test the hypothesis that manganese exposure may change the binding affinity of iron regulatory proteins (IRPs) to mRNAs encoding transferrin receptor (TfR), thereby influencing iron transport at the blood–CSF barrier. A primary culture of choroidal epithelial cells was adapted to grow on a permeable membrane sandwiched between two culture chambers to mimic blood–CSF barrier. Trace ^{59}Fe was used to determine the transepithelial transport of iron. Following manganese treatment (100 μM for 24 h), the initial flux rate constant (K_i) of iron was increased by 34%, whereas the storage of iron in cells was reduced by 58%, as compared to controls. A gel shift assay demonstrated that manganese exposure increased the binding of IRP1 and IRP2 to the stem loop-containing mRNAs. Consequently, the cellular concentrations of TfR proteins were increased by 84% in comparison to controls. Assays utilizing RT-PCR, quantitative real-time reverse transcriptase-PCR, and nuclear run off techniques showed that manganese treatment did not affect the level of heterogeneous nuclear RNA (hnRNA) encoding TfR, nor did it affect the level of nascent TfR mRNA. However, manganese exposure resulted in a significantly increased level of TfR mRNA and reduced levels of ferritin mRNA. Taken together, these results suggest that manganese exposure increases iron transport at the blood–CSF barrier; the effect is likely due to manganese action on translational events relevant to the production of TfR, but not due to its action on transcriptional, gene expression of TfR. The disrupted protein–TfR mRNA interaction in the choroidal epithelial cells may explain the toxicity of manganese at the blood–CSF barrier.

Keywords: Manganese (Mn); Iron (Fe); Influx; Choroid plexus; Z310 cells; Blood–CSF barrier (BCB); Transferrin receptor (TfR); Ferritin; Heterogeneous nuclear RNA (hnRNA); Iron regulatory protein (IRP); Iron response element (IRE); Nuclear run-off assay; Gel shift assay; Reverse transcriptase polymerase chain reaction (RT-PCR); Quantitative real-time RT-PCR

Introduction

Abnormal metabolism of iron in the systemic circulation and in the central nervous system (CNS) is reportedly associated with the etiology of a number of neurodegenerative diseases (Berg et al., 2001; Double et al., 2000; Gerlach et al., 2003). Cellular iron overload in the basal ganglia, particularly in the substantia nigra, may catalyze the generation of reactive oxygen species and enhance lipid peroxidation. This iron-mediated oxidative stress may lead to the degeneration of nigrostriatal dopamine neurons in idiopathic Parkinson's disease patients (Jenner, 2003; Loeffler et al., 1995; Yantiri and Andersen, 1999; Youdim, 2003).

Under normal physiological conditions, the CNS iron homeostasis is balanced by mechanisms that control the influx (i.e., a transferrin receptor [TfR]-mediated process), the storage (i.e., a ferritin-mediated process), and the efflux of iron (i.e., the bulk CSF flow) (Connor and Benkovic, 1992; Deane et al., 2004; Jefferies et al., 1984). The TfR is

* Corresponding author. Fax: +1 765 496 1377.
E-mail address: wzheng@purdue.edu (W. Zheng).

0041-008X/$ - see front matter © 2004 Elsevier Inc. All rights reserved.
doi:10.1016/j.taap.2004.10.003

located at the blood–brain barrier and the blood–CSF barrier, where it is responsible for the fluxes of iron in and out of brain; it also presents on the cell surface of neurons and neuroglia for cellular iron uptake (Burdo and Connor, 2001; Moos and Morgan, 2000). TfR is abundantly expressed in the choroid epithelia (Giometto et al., 1990; Kissel et al., 1998). At the cellular level, the proteins associated with iron homeostasis are post-transcriptionally regulated by binding or unbinding of iron regulatory proteins (IRPs) to mRNAs encoding TfR and ferritin whose sequences contain stem-loop structures, known as iron-responsive elements (IREs) (Beinert and Kennedy, 1993; Klausner et al., 1993). In the absence of iron, IRPs are converted to the high-affinity binding state. The binding of IRPs to the IREs in the 5′ UTR of ferritin mRNA represses the translation of ferritin, while the binding of IRPs to the IREs in the 3′ UTR of TfR mRNA stabilizes the transcripts against as yet undefined ribonucleases. The up-regulation of TfR and down-regulation of ferritin thus elevate the intracellular free iron (Mikulits et al., 1999; Ponka and Lok, 1999).

Research from this laboratory indicates that manganese-induced neurodegenerative damage is associated with an altered iron status in blood circulation as well as in cerebrospinal fluid (CSF) (Zheng and Zhao, 2001; Zheng et al., 1999b). There appeared to be a unidirectional influx of iron from the systemic circulation into the cerebral compartment (Zheng et al., 1999b). Using dual-perfusion technique and capillary depletion method to study iron influx to the brain, we recently further demonstrated that manganese exposure significantly augmented the influx of ^{59}Fe to the choroid plexus, a tissue where the blood–CSF barrier is located, but it did not affect the influx of ^{59}Fe to the other brain regions examined (Deane et al., 2002). Thus, the choroid plexus (and therefore the blood–CSF barrier) may serve as the site for abnormal CNS iron homeostasis following manganese intoxication (Zheng et al., 2003).

Since manganese shares many structural, biochemical, and physiological similarities to iron (Rao et al., 2003; Zheng, 2001), the mechanism of manganese action may result from its direct interaction with iron on enzymes or proteins that require iron as a cofactor in their active catalytic centers. For example, IRP1, also known as cytoplasmic aconitase (ACO1), possesses a [4Fe-4S] cubic active binding site. Increased cellular manganese may replace the fourth labile iron and change IRP1 to [3Fe-4S] configuration; the latter favors the binding of IRP1 to IRE-containing mRNAs (Zheng and Zhao, 2001). Such an action, while suppressing the enzyme's catalytic function, may increase the binding of the protein to the TfR mRNA and subsequently enhance the cellular production of TfR.

Our previous work has demonstrated that manganese exposure inhibits aconitase activity, increases the stability of TfR mRNAs, and promotes the cellular overload of iron in the choroid plexus (Zheng and Zhao, 2001; Zheng et al., 1998a, 1999b). However, it was unclear whether manganese treatment altered the binding affinity of IRPs to IRE-containing mRNAs in the choroidal epithelial cells. It was also unclear whether manganese treatment modulated TfR gene expression at the transcriptional regulatory level. It should be pointed out that manganese action, either to enhance the transcription of TfR or to retard degradation of TfR mRNA, or both, could lead to an increased cellular level of TfR and the ensuing cellular overload of iron.

The purpose of this study was to (1) determine whether manganese exposure alters iron transport by the blood–CSF barrier by using a Transwell transport model with primary culture of choroidal epithelial cells; (2) determine the effect of manganese on the binding affinity of IRPs to IRE-containing mRNAs using a gel shift assay; (3) determine cellular mRNA levels and protein levels of TfR as affected by manganese treatment; (4) determine whether manganese exposure altered the transcriptional gene expression of TfR by determining the levels of heterogeneous nuclear RNA (hnRNA) encoding TfR and the nascent TfR mRNA; and (5) determine whether cellular mRNA levels of iron storage protein ferritin were affected by manganese exposure by using RT PCR and quantitative real-time RT-PCR.

Materials and methods

Primary culture of choroidal epithelial cells and Transwell transport studies. A primary culture of choroidal epithelial cells, which was used in the Transwell transport study, was established by using the method previously published (Zheng et al., 1998b). Permeable membranes attached to the Transwell-COL culture wells were pretreated with laminin (14 μg/mL) for 10 min. Aliquots (0.5 mL) of cell suspension were plated in 12-mm wells (2×10^5 cells/well), which were designated as the inner chamber. The epithelial cells formed an impermeable monolayer barrier after 6–7 days in the culture. The formation of the cellular "barrier" between two chambers was confirmed by measurement of *trans*-epithelial electrical resistance (TEER) and by determination of paracellular leakage of [^{14}C]sucrose according to previously established criteria by this laboratory (Zheng and Zhao, 2002a, 2002b).

Mn(II) solution as $MnCl_2$ was prepared by directly dissolving $MnCl_2$ in distilled, deionized water at a concentration of 40 mM as the stock solution, which was autoclaved prior to the use. The working solutions were diluted from the stock on the day of use.

The cells were exposed to 100 μM of $MnCl_2$ in culture medium of both chambers for 3 days prior to transport study. For ^{59}Fe transport, the cells were washed with and cultured in a serum-free Dulbecco's modified Eagle's medium (DMEM) supplemented with 5 μg/mL insulin, 5 μg/mL transferrin, 5 ng/mL sodium selenite, 5 ng/mL fibroblast growth factor, 25 μg/mL prostaglandin E1, and 10 ng/mL mouse epithelial growth factor (EGF). ^{59}Fe was added to the donor (outer) chamber to a final concentration

of 1.5 μM (0.18 μCi/mL). Aliquots (10 μL) of media in both chambers were removed at specified times and counted in a gamma counter.

The initial flux rate constant (K_i) was estimated from the regression slope of initial 4 data points (0–7 h). The steady state concentration (C_{ss}) was calculated based on the mean values of the last 3 data points (26–44 h). The area under the curve (AUC) was obtained from the data points between 0 and 44 h.

Culture of choroidal epithelial Z310 cell line and manganese treatment. A choroidal epithelial Z310 cell line was originally developed by this laboratory (Zheng and Zhao, 2002b). The cells possess the typical morphology of choroidal epithelial type and express the marker of transthyretin. Moreover, the cell line retains the proteins involved in cellular iron regulation such as TfR and ferritin. This cell line was used in the subsequent experiments to investigate mechanisms of manganese–iron interaction.

Z310 cells were grown in DMEM supplemented with 10% FBS, 100 units/mL penicillin, 100 μg/mL streptomycin, and 10 mg/mL Gentamicin solution in 100 mm Petri plates in a humidified incubator with 95% air–5% CO_2 at 37 °C. Culture medium was changed twice per week.

The cells were exposed to manganese in culture media at the concentrations of 50, 100, or 200 μM. To create iron deficiency and overloaded conditions, cells were cultured in a medium containing 50 μM of desferroxamine (DFOM) and 30 μM of hemin for 10 h, respectively. The cells were harvested at the designated times and processed according to the procedures described below.

Western blot analysis of TfR. Proteins were extracted from cultured Z310 cells and total protein content was measured by a Bio-Rad protein assay kit using bovine serum albumin (range: 12.5–100 μg/mL) as the standard. Aliquots (20 μg) homogenates were loaded onto a 4–20% Tris–HCl linear gradient ready gel (Bio-Rad), electrophoresed, and then transferred onto a PVDF membrane. Membranes were immunoblotted with mouse anti-human TfR antibody at room temperature for 60 min, followed by incubation with peroxidase-labeled anti-mouse secondary antibody. The bands corresponding to TfR (95 kDa) were visualized using an ECL method (Amersham, Piscataway, NJ). β-actin (42 kDa) was used as an internal control. Band intensity was quantified using UN-SCAN-IT (Version 5.1) software (Silk Scientific Inc., Orem, UT).

Gel shift assay. A gel shift assay was conducted to determine the interaction between IRPs and mRNAs containing IRE as described in literature (Lin et al., 2001). The procedure consisted of three major steps. (1) Extraction of S100 cytoplasmic protein: Z310 cells with or without manganese exposure were harvested and homogenized, followed by centrifugation at 100,000 × *g* for 1 h. The supernatant was dialyzed for 8 h against 20 volumes of degassed dialysis buffer composed of 20 mM HEPES, 0.1 M KCl, 20% (v/v) glycerol, 0.2 mM EDTA, 0.5 mM PMSF, and 0.5 mM dithiothreitol (DTT) using Spectra/Pro 96-well MicroDialyzer (150 μL capacity, Spectrum Laboratories, Rancho Dominguez, CA). The S100 cytoplasmic extracts were stored at −80 °C until use.

(2) Preparation of RNAs containing stem-loop structure: the DNA oligonucleotide template T7-1 (sequence: 5′ TAA TAC GAC TCA CTA TA 3′) was annealed to ferritin-IRE (Ft-IRE, 2 μM) (sequence: 5′ GGA TCC GTC CAA GCA CTG TTG AAG CAG GAT CCT CTC CCT ATA GTG AGT CGT ATTA) (customer synthesized by IDT, Coralville, IA) in 50 μL anneal buffer (10 mM Tris–HCl pH 7.5 and 10 mM $MgCl_2$). The mixture was heated to and maintained at 95 °C for 5 min and then cooled to less than 35 °C before operating the next step. The transcription reaction was carried out in a total of 50 μL with 0.2 μM annealed template, 12.5 U T7 RNA polymerase, 2 mM each of ATP, GTP, and CTP, 30 μM UTP, and 0.33 μM [α-^{32}P]UTP for 3.5 h at 37 °C, followed by RNA precipitation. The labeled RNA was further purified on a 15% denatured polyacrylamide gel. The bands corresponding to transcription products were excised and eluted; the RNA was recovered, precipitated, and then resuspended in water to at least 10,000 cpm/μL. The products of RNAs containing ferritin stem-loop structure were frozen at −80 °C until use (Lin et al., 2001).

(3) Gel shift assay: the S100 cytoplasmic extracts (40 μg of protein) were incubated with an excess (0.2 ng, 10^5 cpm) of [^{32}P]-labeled IRE-containing RNA in a band shift buffer (10 mM HEPES, pH 7.6, 3 mM $MgCl_2$, 40 mM KCl, 5% glycerol and 1 mM DTT) at 20 °C for 30 min (Leibold and Munro, 1988). One unit of RNase T1 and 5 mg/mL heparin were added to destroy the unprotected RNA and to minimize nonspecific protein–RNA interaction. The mixtures were then loaded on 4% non-denature polyacrylamide gels and visualized by autoradiography. The density of protein–RNA bound bands was quantified.

Reverse transcriptase PCR (RT-PCR)-based transcriptional assay of heterogeneous nuclear RNA (TfR hnRNA assay). Quantitation of the primary transcripts, which are the very first products (i.e., hnRNA) of transcription including both introns and extrons, allows one to decipher whether or not manganese exposure has a direct effect on gene expression at the transcriptional level. Total RNA was extracted from Z310 cells using RNeasy mini kit (Qiagen, Valencia, CA). One μg of total RNA was reverse-transcribed with a RETROscript kit (Ambion, Austin, TX), for rat TfR hnRNA using a forward primer 5′ TAA GGC AAA ACA GGT CCC AT-3′ and reverse primer 5′ TAA ATC CCC AAC CCA AGC TA-3′ , which yielded a 446-bp product, designed based on Intron I (base 13–975) of Rattus norvegicus transferrin receptor(14907 bp, NCBI access #: NW_047356**),** and for rat β-actin hnRNA, an internal marker, using a forward primer 5′ CAC TGT CGA GTC

CGC GTC CAC-3′ and a reverse primer 5′ GGA ATA CGA CTG CAA ACA CTC-3′ to produce a 258-bp product (Danzi et al., 2003). The products were amplified by PCR with 38 cycles: melting step at 94 °C for 30 s, annealing at 54 °C for 30 s, and extension at 72 °C for 40 s. Aliquots of the PCR reaction products were run on a 1.2% agarose gel containing ethidium bromide. The density of bands corresponding to TfR hnRNA and β-actin hnRNA were quantified using UN-SCAN-IT software.

Nuclear run-off assay. A nuclear run-off assay as described by Pastorcic and Das (2002) was employed with some modifications to determine the rate of transcription of TfR genes as affected by manganese exposure. The experiment consisted of three steps. (1) Preparation of cDNA membranes: cDNAs designed for TfR, GAPDH and S15 were immobilized onto a Zeta-Probe genomic tested blotting membrane (Bio-Rad Laboratories) by using a UV Cross-linker (UVP, Upland, CA). The targeted TfR cDNA and the loading controls (cDNAs of GAPDH and S15) were obtained by RT-PCR with a RETROscript kit, for rat TfR, using a forward primer 5′ GGA TCA AGC CAG ATC AGC ATT-3′ and reverse primer 5′ CCA TCA ATC GGA TGC TTT ACG-3′, which yielded a 1554-bp product; for rat GAPDH, using a forward primer 5′ AGA CAA GAT GGT GAA GGT CGG-3′ and reverse primer 5′ GGG TGC AGC GAA CTT TAT TG-3′, providing a 1208-bp product; and for S15, using a forward primer 5′ TTC CGC AAG TTC ACC TAC C-3′ and reverse primer 5′ CGG GCC GGC CAT GCT TTA CG-3′ to generate a 361-bp product.

(2) Preparation of ^{32}P-labeled nascent nuclear RNA: At the end of the 24-h treatment with 100 μM of $MnCl_2$, Z310 cells were harvested and resuspended (10^7–10^8 cells) in 2 mL of 10 mM Tris (pH 7.4), 3 mM $CaCl_2$, 2 mM $MgCl_2$, and 1% NP-40. After homogenization, the nuclei were pelleted after a brief spin at 2000 rpm for 5 min at 4 °C. The isolated nuclei were resuspended in 200 μL of 50 mM Tris (pH 8.3), 5 mM $MgCl_2$, 0.1 mM EDTA and 40% (v/v) glycerol per 5×10^7 nuclei, and stored at −80 °C until use. The transcription reactions were started by adding an equal volume of 10 mM Tris (pH 8), 5 mM $MgCl_2$, 0.3 M KCl, 1 mM ATP, 1 mM CTP, 1 mM GTP, and 5 mM DTT to the nuclei suspension with 100 μCi [α-^{32}P]UTP (3000 Ci/mmol). The mixture was incubated for 30 min at 30 °C with agitation at 150 rpm. Reactions were stopped by adding 600 μL of HSB buffer containing 0.5 M NaCl, 50 mM $MgCl_2$, 2 mM $CaCl_2$, 10 mM Tris (pH 7.4), and 1000 U of RNase-free DNase I. DNase I treatment, which eliminates unwanted DNA sequences, was stopped by adding 200 μL 5% (w/v) SDS in 0.5 M Tris, pH 7.4, and 0.125 M EDTA and 10 μL of 20 mg/mL proteinase K. After 30 min incubation at 42° C, the elongated ^{32}P-labeled nascent nuclear RNAs were extracted with phenol/chloroform/isoamyl alcohol (25:24:1, v/v/v). The RNAs were precipitated by adding 2 mL ice-cold H_2O containing 10 μL of 10 mg/mL yeast tRNA and 3 mL of 10% trichloroacetic acid (TCA)/60 mM sodium pyrophosphate. After incubation on ice for 30 min, the precipitates were collected by filtration onto Whatman GF/A glass fiber filters. Filters were washed three times with 10 mL of 5% TCA/30 mM sodium pyrophosphate and transferred to vials containing 1.5 mL of 20 mM HEPES (pH 7.5), 5 mM $MgCl_2$, 1 mM $CaCl_2$ and 1000 U of RNase-free DNase I. After 30 min treatment at 37 °C, the reactions were quenched with 50 μL of 0.5 M EDTA and 70 μL of 20% SDS, and the samples were heated at 65 °C for 10 min, followed by centrifugation. The supernatant was transferred, treated with proteinase K for 30 min at 37 °C, and extracted again with an equal volume of phenol/chloroform/isoamyl alcohol (25:24:1). The RNAs were precipitated with 0.3 M sodium acetate and 100% ethanol overnight at −20 °C. RNA pellets were resuspended in 1 mL of 10 mM N-tris(hydroxymethyl)methyl-2-aminoethanesulfonic acid (TES), pH 7.4, 0.2% SDS and 10 mM EDTA.

(3) Hybridization: The ^{32}P-labeled nascent nuclear RNA samples were spotted onto Whatman GF/F glass fiber filters and counted for radioactivity so to adjust the radioactivity to exceed 5×10^6 cpm/mL. The RNA samples were added to a vial containing the same buffer. Membrane strips bearing cDNAs from the first step were immersed in radiolabeled RNA samples and hybridized at 65 °C for 48 h. The membrane strips were removed, washed with 2 × SSC for 20 min, and autoradiographed for quantitation.

RT-PCR analysis of light chain-ferritin (LFt) and heavy chain-ferritin (HFt). Two micrograms of total RNA was reverse-transcribed with a RETROscript kit, for rat LFt using a forward primer 5′ -AGA AGC CAT CTC AAG ATG AG-3′ and reverse primer 5′ -CTA GTC GTG CTT CAG AGT GA-3′, which yielded a 304-bp product and for rat HFt using a forward primer 5′ -CCA GTA AAG TCA CAT GGC CT-3′ and reverse primer 5′ -GGC TAC TGA CAA GAA TGA TC-3′, which yield a 221-bp product (Marton et al., 2000). Rat GAPDH was used as an internal control with a forward primer 5′ -CAC CAC CCT GTT GCT GTA-3′ and reverse primer 5′ -TAT GAT GAC ATC AAG AAG GTG G-3′ (David et al., 2001) to generate a 219-bp product.

The products of LFt and HFt were amplified by PCR with 28 cycles: melting step at 94 °C for 40 s, annealing at 53 °C for 30 s, and extension at 72 °C for 45 s. The products of GAPDH was amplified by PCR with 35 cycles: melting step at 94 °C for 40 s, annealing at 54 °C for 30 s, and extension at 72 °C for 45 s. Aliquots of the PCR reaction products were run on a 1.5% agarose gel containing ethidium bromide. The density of bands corresponding to LFt and HFt were normalized by GAPDH and quantified using UN-SCAN-IT software.

Quantitative real-time RT-PCR analysis TfR hnRNA, TfR mRNA, and ferritin mRNA. Levels of TfR hnRNA, TfR mRNA and ferritin (heavy chain and light chain) mRNA were quantified using real-time RT-PCR analysis as

described by Walker (2001). Briefly, total RNA was isolated from Z310 cells using TRIzol reagent (Invitrogen, Carlsbad, CA), followed by purification on RNeasy columns (Qiagen, Palo Alto, CA). Purified 1 μg of RNA was reverse transcribed with MuLV reverse transcriptase (Applied Biosystems, Foster City, CA) and oligo-dT primers. The forward and reverse primers for selected genes were designed using Primer Express 2.0 software (Applied Biosystems). The ABsolute QPCR SYBR green Mix kit (ABgene, Rochester, NY) was used for real-time PCR analysis. The amplification was carried out in the Mx3000P real-time PCR System (Stratagene, La Jolla, CA). Amplification conditions were 15 min at 95 °C, followed by 40 cycles of 30 s at 95 °C, 1 min at 55 °C (for TfR hnRNA) or 60 °C and 30 s at 72 °C.

Primers sequences used for real-time RT-PCR analysis were: in hnRNA assay, for rat TfR hnRNA, using a forward primer 5′ CAG GAA GTA GAA ACC CTA GAA AGG-3′ and reverse primer 5′ TGC AAT AGT CGC AAA GCA GA-3′ , the fragment crosses intron I and extron II of rat TfR (the gene was deposited in BCBI, gi:34869631), and for rat β-actin hnRNA, an internal marker, using a forward primer 5′ CAC TGT CGA GTC CGC GTC CAC-3′ and a reverse primer 5′ GGA ATA CGA CTG CAA ACA CTC-3′ ; in mRNA measurement, for rat TfR using a forward primer 5′ -CTA GTA TCT TGA GGT GGG AGG AAG AG-3′ and reverse primer 5′ -GAG AAT CCC AGT GAG GGT CAG A-3′ (Genebank Access No. M58040), for rat LFt using a forward primer 5′ -GTG AAC CGC CTG GTC AAC TT-3′ and reverse primer 5′ -AAC CCG AGC TAC TCA CCA GAG A-3′ (Genebank Access No. J02741), for rat HFt using a forward primer 5′ -CAA GTG CGC CAG AAC TAC CA-3′ and reverse primer 5′ -GTG TCC CAG GGT GTG CTT GT-3′ (Genebank Access No. M18051); for rat GAPDH, used as an internal control, using a forward primer 5′ -CCT GGA GAA ACC TGC CAA GTA T-3′ and reverse primer 5′ -AGC CCA GGA TGC CCT TTA GT-3′ (Genebank Access No. NM_017008).

The relative differences in gene expression between groups were expressed using cycle time (Ct) values; these Ct values of the interested genes were first normalized with that of β-actin or GAPDH in the same sample, and then the relative differences between control and treatment groups were calculated and expressed as relative increases setting the control as 100%. Assuming that the Ct value is reflective of the initial starting copy and that there is 100% efficiency, a difference of one cycle is equivalent to a two-fold difference in starting copy (Liu et al., 2004a, 2004b; Walker, 2001).

Statistical analysis. All data are expressed as mean ± SD. The replicates of experiments conducted in the same day were referred as $n = 1$; three such replicates on different dates were used for statistical analyses. The statistical analyses were carried out by paired t testing for single comparison or by analysis of variance (ANOVA), where the multiple comparison was required. Data presented in Fig. 1 were analyzed by two-way ANOVA to determine the overall treatment effect using GB-Stat PPC 5.4.6 package. The linear regression analysis was performed by SPSS 12.0 statistic package for Windows.

Materials. Chemicals were obtained from the following sources: mouse EGF, DMEM, Hanks' balanced salt solution (HBSS), RNase-free DNase I, 0.25% Trypsin–1 mM EDTA (TE) and yeast tRNA from Invitrogen Life Technologies; RNase T1, pronase, *cis*-hydroxyproline from Calbiochem (San Diego, CA); mouse anti-human TfR antibody from ZYMED (San Francisco, CA); ATP, GTP, CTP, and UTP (NTPs), [α-^{32}P]UTP, proteinase K, peroxidase-labeled anti-mouse secondary antibody from Amersham; low protein binding filter units (Millex-GV4, 0.22μm) from Millipore (Bedford, MA); ^{59}Fe (18.7 mCi/mg) from NEN Life Products (Boston, MA); deferoxamine mesylate (DFOM), hemin, tetramethyl-ethylenediamine (TEMED), fetal bovine serum (FBS) and all other chemicals from Sigma (St. Louis, MO). All reagents were of analytical grade, HPLC grade or the best available pharmaceutical grade.

Results

Manganese exposure increases transport of iron by choroidal epithelial cells

Following 1-week culture of primary choroidal epithelial cells on a porous membrane in the inner chamber, a cell monolayer was formed with a TEER value between 80 and

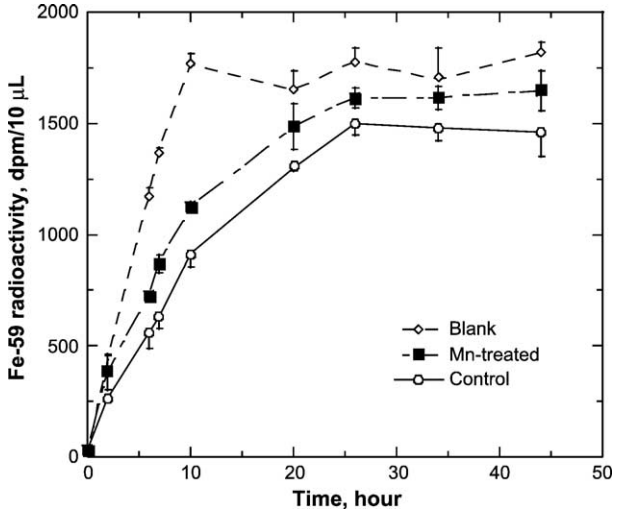

Fig. 1. Mn exposure facilitated Fe transport by the blood–CSF barrier. Fe transport study was conducted using an in vitro Transwell device with primary choroidal epithelial cells. Cells were exposed to 100 μM Mn for 3 days. ^{59}Fe was added into the donor chamber and the radioactivity was monitored in the acceptor chamber at time indicated. Data represent mean ± SD, $n = 3$.

Table 1
Kinetic parameters of iron transport at the blood–CSF barrier as affected by manganese exposure

	Blank	Control	Mn-Treated	% Increase[a]
K_i (dpm/mL/min)	188.9 ± 3.93	81.4 ± 8.15	109.1 ± 7.27**	34%
C_{ss} (dpm/10 μL)	1713 ± 101	1458 ± 109	1615 ± 107*	11%
$AUC_{0-44\ h}$ (dpm × 10^3/10 μL h)	67.7 ± 0.37	50.6 ± 1.65	58.3 ± 2.08**	15%

Blank: in absence of cells in the chamber; Control: in presence of cells without manganese treatment; Mn-treated: in presence of cells with manganese treatment at 100 μM for 3 days.
[a] Values in Mn-treated groups as % increase of controls. Date represent mean ± SD (n = 3).
* $P < 0.05$.
** $P < 0.01$, as compared to controls.

120 Ω cm^2 (Zheng and Zhao, 2002a, 2002b). The permeability coefficient of [^{14}C]sucrose on the Transwell model was less than 3 × 10^{-3} cm/min, which is comparable to reports in literature (Johnson and Anderson, 1999; Lagrange et al., 1999).

This in vitro model of blood–CSF barrier was used to study the effect of manganese exposure on iron transport at the blood–CSF barrier. When ^{59}Fe was added into the donor (outer) chamber, the radioactivity in the acceptor (inner) chamber raised gradually. A two-way ANOVA revealed a significant treatment effect between Mn-treated group and control group ($P < 0.0001$), between the blank (without cells) and controls (with cells) ($P < 0.0001$), and between the blank and Mn-treated group ($P < 0.0001$). The initial flux rate constant (K_i) in the control, untreated cells was 81 dpm/mL/min. Exposure of the cells to manganese (100 μM for 3 days) increased K_i to 109 dpm/mL/min, an increase of 34% (Fig. 1). The steady-state concentration (C_{ss}) and AUC_{0-44} of ^{59}Fe in the inner chamber was increased by 11% and 25% of controls, respectively (Table 1).

When the cells in the inner chamber were harvested to determine the retention of ^{59}Fe in the choroidal epithelial cells, it was found that manganese exposure significantly reduced the amounts of ^{59}Fe retained in cells by 58% of controls (Fig. 2). These data suggested that while manganese treatment facilitated iron transport at blood–CSF barrier, it reduced the iron storage by these cells.

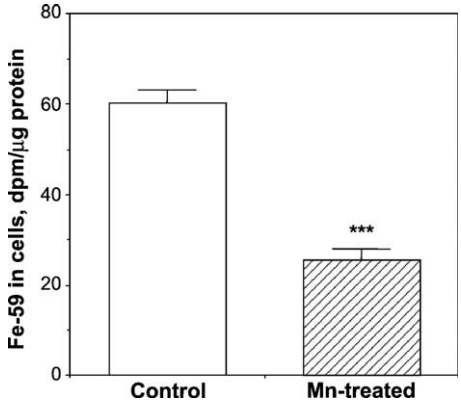

Fig. 2. Mn exposure reduced Fe storage in primary choroidal epithelial cells. Cells on the chamber membrane were collected and counted for radioactivity. Data represent mean ± SD, n = 3. ***$P < 0.001$.

Manganese exposure increases the expression of TfR in vitro

Facilitated transport of iron by the choroidal epithelial barrier after manganese treatment could result from an elevated cellular TfR. Quantitative real-time RT-PCR revealed that manganese treatment at both 100 and 200 μM for 24 h significantly increased the levels of TfR mRNA by 67% and 90%, respectively ($P < 0.01$, Fig. 3). By using Western blot analysis, a significant increase in cellular protein levels of TfR was also found in choroidal epithelial Z310 cells following manganese exposure at 100 μM (Fig. 4A). The increase in TfR levels was evident at 12 h after exposure ($P < 0.05$) and it reached the maximum (84% increase) at 36 h (Fig. 4B). The effect remained significant even at day 6 after manganese exposure ($P < 0.05$). Within the dose range of 50–200 μM of $MnCl_2$ in the culture media, there was a significant dose–response relationship between manganese concentrations and TfR protein expression by linear regression analysis (r^2 = 0.542, p = 0.006) (Fig. 4C).

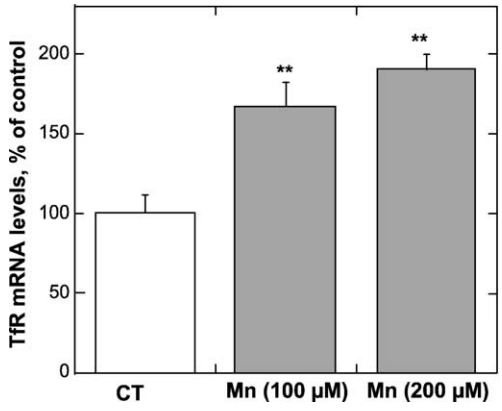

Fig. 3. Mn exposure increased the level of TfR mRNA in choroidal epithelial Z310 cells by quantitative real time RT-PCR. Z310 cells were exposed with 100 or 200 μM of Mn for 24 h. Total RNAs were extracted and reverse-transcripted to cDNA for amplifications. Relative differences between groups were analyzed using cycle time values; these values were initially normalized with that of GAPDH in the same sample followed by expression as a percentage of controls. Data represent mean ± SD, n = 3. **$P < 0.01$ (compared to controls).

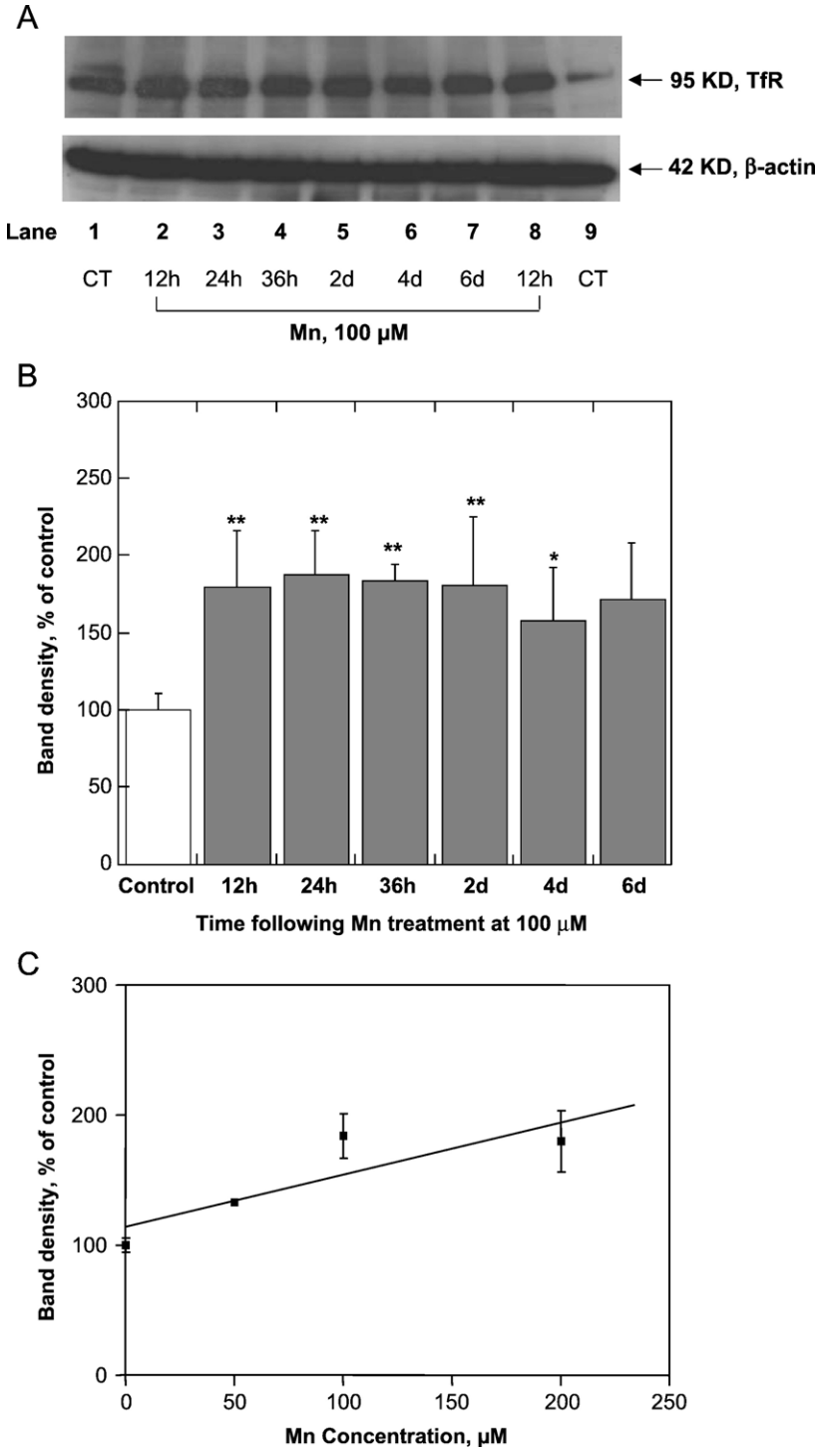

Fig. 4. Mn exposure increased the level of TfR protein in choroidal epithelial Z310 cells by Western blot analyses. Z310 cells were exposed with 100 μM of Mn for the durations as indicated. (A) A typical blot of triplicate experiments. CT: control cells; Mn: Mn-treated cells; β-actin: serving as a loading control. (B) Time course study. The band densities were normalized by β-actin and expressed as % of controls. Data represent mean ± SD, $n = 3$. *$P < 0.05$, **$P < 0.01$ as compared to controls. (C) Dose–response study. Cells were exposed to Mn at 50, 100, or 200 μM for 36 h. Data represent mean ± SD, $n = 3$, correlation coefficient ($r^2 = 0.542$, $P < 0.01$).

Manganese exposure increases IRP binding to TfR mRNA in vitro

The increased protein level of TfR by manganese treatment could be either due to an up-regulation of TfR gene expression at the transcriptional level, or due to a stabilized protein expression at the translational level. Since TfR mRNA possesses a unique stem-loop structure for IRP binding, a gel shift assay was performed to determine if manganese treatment enhanced the binding of cytosolic

IRPs to radiolabeled TfR mRNA. At a concentration of 100 μM, manganese exposure caused an increase of binding of IRPs to the stem loop-containing mRNAs (Fig. 5A). The binding of IRP1 to IRE-containing mRNAs reached the highest at 24 h following manganese exposure ($P < 0.05$, Fig. 5B); the time course appeared to be parallel to that of TfR protein synthesis (Fig. 4B). Manganese treatment also promoted the binding of IRP2 to IRE-containing mRNA. Application of DFOM (50 μM for 10 h), an iron chelator which depletes cellular iron, increased the binding of IRP1, but not IRP2, to IRE-containing mRNAs by 155% (Figs. 5A, B).

Effect of manganese exposure on the status of TfR hnRNA

The hnRNA consists of newly transcribed, unspliced nuclear RNAs prior to their entry to cytoplasm. The levels of hnRNA reflect the combination of the rate of gene transcription, the status of RNA processing, and the stability of nuclear RNA (Delany, 2001). To investigate whether manganese exposure directly affected the transcription of TfR gene. The relative amounts of the 446-bp TfR hnRNA and quantitation of 375-bp TfR hnRNA level in 1 μg of total RNA extracted from Z310 cells were determined by using RT PCR and real time PCR, respectively. The amount of TfR hnRNA was normalized by the expression of β-actin hnRNA. Results in Fig. 6 showed that manganese treatment (100 and 200 μM for 24 h) did not cause any statistically significant changes in the expression of TfR hnRNA as compared to the control group.

Effect of manganese exposure on transcription rate of nascent TfR RNA

Nuclear run-off assay allows specifically for detection of changes in the transcription rate of nascent RNA. In this experiment, the nuclei from Z310 cells, which were exposed to 100 μM of manganese for 24 h, were harvested; the transcripts that had already been initiated within the nuclei at the time of harvest were further elongated in the presence of ^{32}P-labeled ribonucleotides. These labeled nascent RNAs were then purified and the levels of TfR mRNAs quantified by hybridization to cDNA probes designed for rat TfR, which were pre-immobilized onto nitrocellulose membrane. Rat GAPDH and S15 cDNA probes were used as internal control. The results from nuclear run-off assay demonstrated that no statistically significant differences were observed between control and manganese-treated groups (Fig. 7). The data suggested that manganese exposure seems unlikely to affect the transcription rate of nascent TfR RNA.

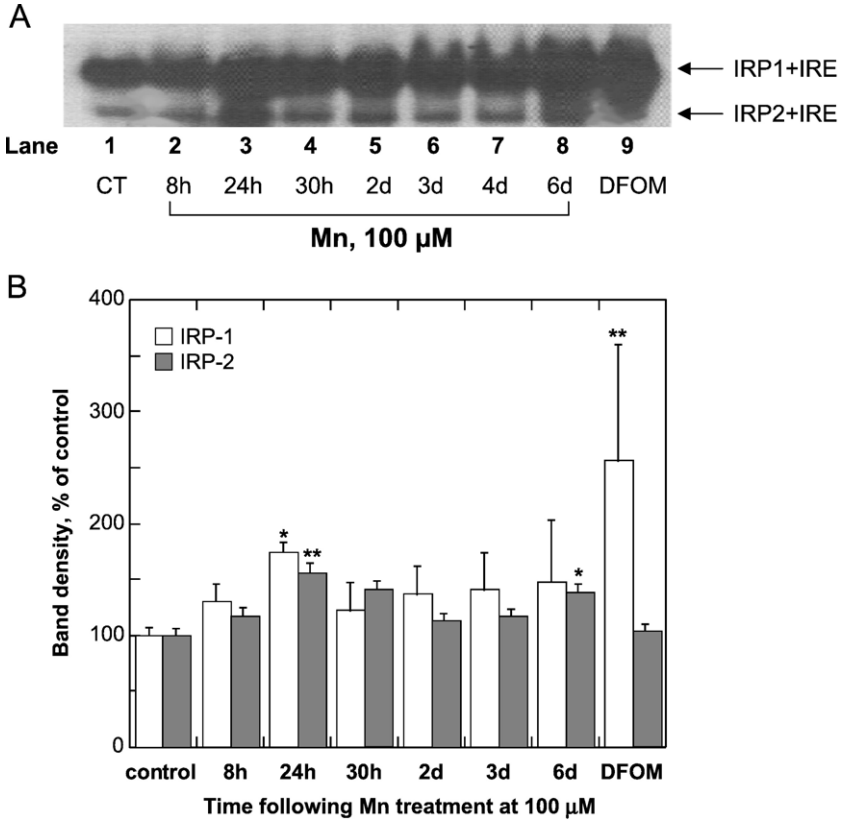

Fig. 5. Mn exposure increased the binding of IRPs to TfR mRNA in choroidal Z310 cells by a gel shift assay. Cytoplasmic protein extracts were incubated with ^{32}P-labeled Ft-IRE; the complexes were separated on non-denatured gel. (A) Data showed a representative autoradiography of three independent experiments. (B) The band densities were quantified and expressed as mean ± SD, $n = 3$. *$P < 0.05$, **$P < 0.01$ as compared to controls.

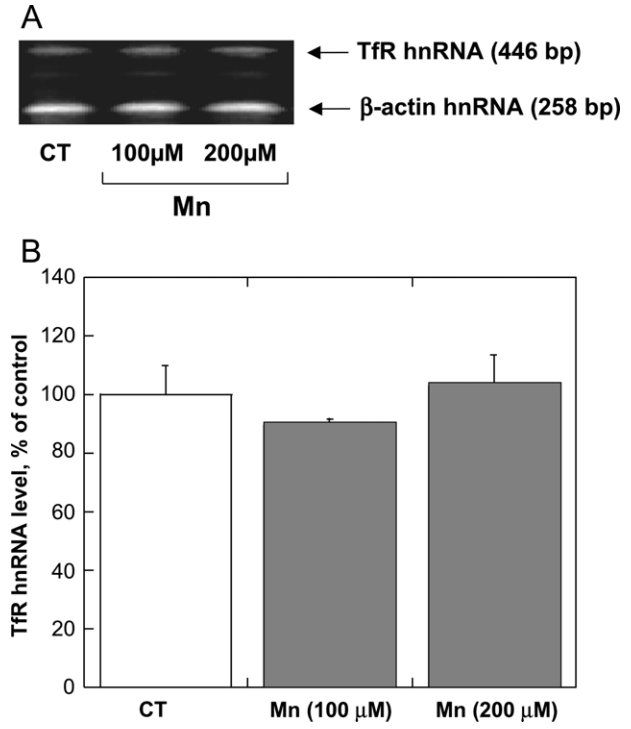

Fig. 6. Analysis of TfR hnRNA in choroidal Z310 cells. (A) RT-PCR assay analysis TfR hnRNA. Cells were treated with 100 or 200 μM of Mn for 24 h. Total RNA extracts were used to determine TfR hnRNA (446 bp) and β-actin hnRNA (258 bp). Data represent a typical autoradiography of three independent experiments. CT: control cells; Mn: Mn-treated cells. (B) Real-time PCR quantification of TfR hnRNA expression in Z310 cells (control and Mn-treated). Relative differences in gene expression between groups were expressed using cycle time values; these values were first normalized with that of β-actin in the same sample, and the expression in the experimental group was expressed as a percentage of expression in controls. Averages of triplicate samples from three independent experiments are shown. Date were expressed as mean ± SD, $n = 3$ ($P > 0.05$).

Manganese exposure decreases intracellular ferritin level in vitro

Since manganese treatment reduced the cellular retention of ^{59}Fe as seen in the Transwell study (Fig. 2), it became necessary to investigate whether manganese exposure altered the cellular level of ferritin. Both RT-PCR analysis (Figs. 8A, B) and real-time PCR (Fig. 8C) revealed that manganese treatment at either 100 or 200 μM for 24 h significantly reduced the levels of ferritin mRNA with the heavy chain being more profoundly affected than the light chain. DOFM (50 μM for 10 h) caused the similar reduction in ferritin levels, whereas the treatment with hemin (30 μM for 10 h) significantly increased the cellular ferritin (Fig. 8).

Discussion

Manganese exposure alters iron homeostasis in systemic circulation and in the CNS. Following manganese exposure, toxicity is thought to be associated with changes of the expression of TfR in the brain barrier systems, that is, the blood–brain barrier and blood–CSF barrier (Zheng, 2001). The cellular level of TfR is regulated at both transcriptional and translational levels. The present work indicates that manganese exposure increases the amount of TfR in cultured choroidal epithelial cells, thereby facilitating the transport of iron at the blood–CSF barrier. We further demonstrate, for the first time in the literature, that the increased TfR concentration in the choroid plexus is due primarily to manganese action at translational level on protein–TfR mRNA interaction, but not due to manganese effect on transcriptional modulation of TfR gene expression.

Our previous studies suggest that manganese exposure selectively increases TfR mRNA in cultured primary choroidal epithelial cells and neuronal type PC12 cells, but not in primary astrocytes (Chen et al., 2001; Zheng and Zhao, 2001). This corresponds to the increase of cellular ^{59}Fe uptake by PC12 cells, but not astrocytes, following Mn exposure (Zheng and Zhao, 2001). Results presented in this report by using quantitative real time RT-PCR and Western blot further corroborate that the increased expression of TfR mRNA by manganese did lead to an increased protein level of TfR in the choroid plexus. The effect of manganese on the expression of cellular TfR was both manganese concentration-dependent and exposure time-related. Thus, alteration of cellular iron homeostasis following manganese exposure appeared to be a direct result of altered cellular TfR expression by manganese.

Regulation of TfR expression occurs at multiple sites, that is, at transcriptional modulation of TfR gene transcription within nuclei or at translational intervention of TfR protein synthesis in cytoplasm. Transcriptional regulation usually affects cellular RNA abundance by affecting the rate of transcription and RNA processing, while post-transcriptional regulation mainly influences the mRNA abundance by acting on the rate of mRNA decay. Thus, an elevated

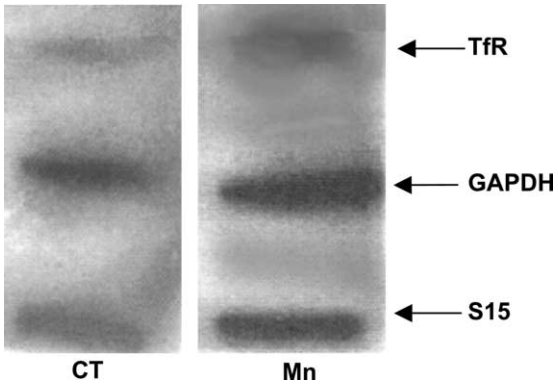

Fig. 7. Nuclear run-off analysis of nascent TfR mRNA in choroidal Z310 cells. Cells were treated with 100 μM of Mn for 24 h. The nuclei were isolated and the nascent mRNA transcripts elongated with labeled [α-^{32}P]UTP. Data represent a typical of autoradiography of three independent experiments. CT: control cells; Mn: Mn-treated cells; GAPDH and S15: used as the loading controls.

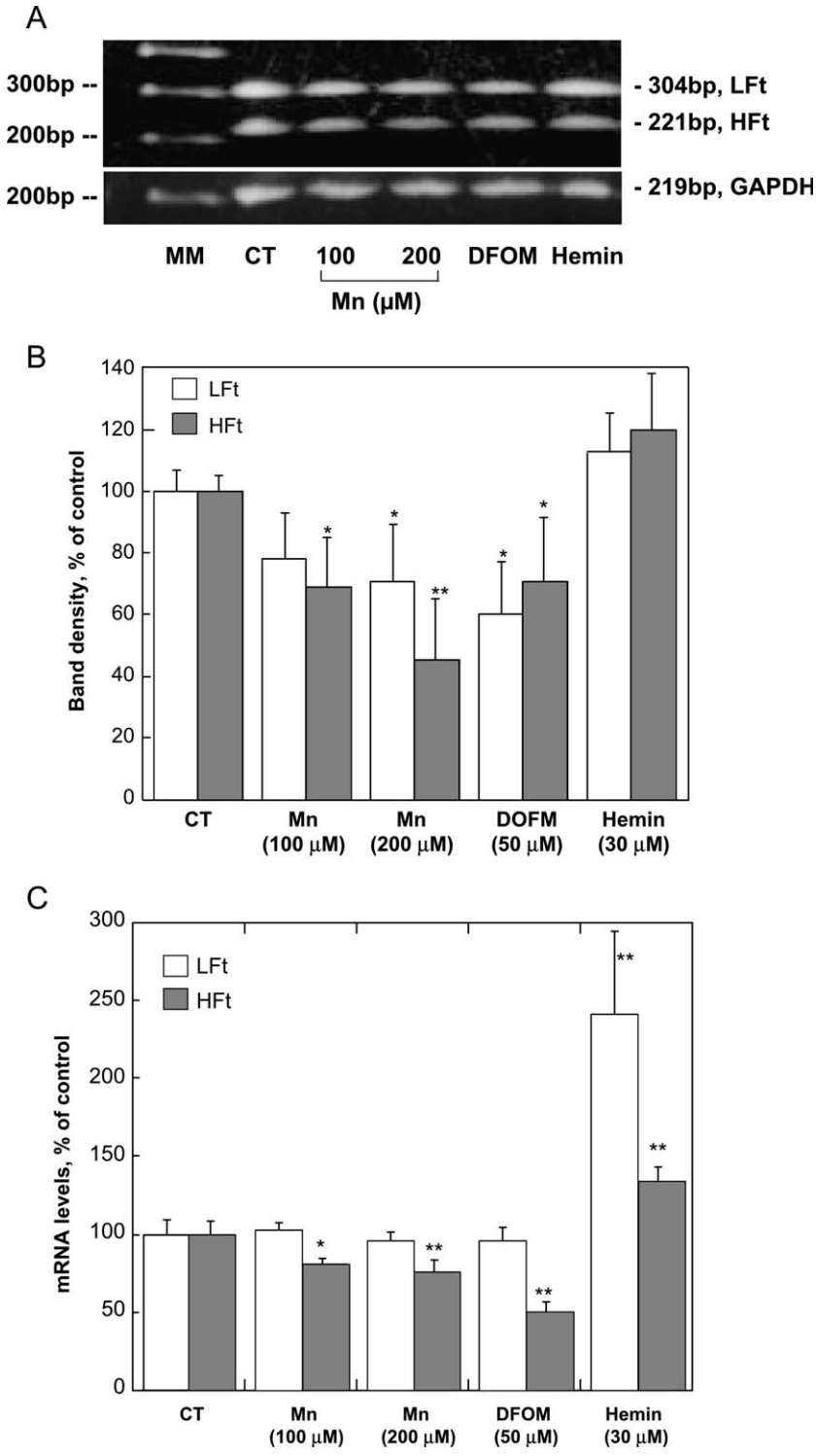

Fig. 8. Mn exposure reduced levels of ferritin mRNA in choroidal epithelial Z310 cells. Z310 cells were exposed with Mn for 24 h, 50 μM DFOM, or 30 μM hemin for 10 h. Total RNA extracts were used for RT-PCR analyses and quantitative real-time PCR measurement. (A) A typical blot of triplicate experiments for RT PCR. MM: molecular marker; CT: control cells; Mn: Mn-treated cells; LFt: ferritin light chain; HFt: ferritin heavy chain. (B) The band densities in RT-PCR were quantified and expressed as mean ± SD, $n = 3$. *$P < 0.05$, **$P < 0.01$ as compared to controls. (C) Real-time PCR quantification of mRNAs encoding light chain ferritin (LFt) and heavy chain ferritin (HFt) in Z310 cells. Relative differences in gene expression between groups were expressed using cycle time values; these values were first normalized with that of GAPDH in the same sample, and the expression in the experimental group was expressed as a percentage of expression in controls. Averages of triplicate samples from three independent experiments are shown. Date were expressed as mean ± SD, $n = 3$. *$P < 0.05$, **$P < 0.01$.

level of TfR mRNA by manganese treatment could result from either a decrease in TfR mRNA degradation, or an increase in TfR mRNA synthesis, or both. Two methods were used in the current research to determine whether manganese acted on the gene transcription of TfR. Quantification of primary TfR transcripts from hnRNA allows for identification of a direct effect of manganese on gene transcription of TfR within nuclei (Delany, 2001). When the nuclear RNA was harvested from both control and manganese-treated groups, no significant changes in TfR hnRNA were found between these two groups. Thus, it is unlikely that manganese exposure activated the transcription of the genes that encode TfR.

The nuclear run-off assay detects the changes in the transcription activity of nascent TfR mRNA (but not changes in processing of TfR RNAs). Following elongation with ^{32}P-labeled ribonucleotides and hybridization onto the filter with an immobilized TfR cDNA probe, the nascent TfR mRNA was quantified by removal (run-off) of nonspecific RNAs by RNase A. Similar to results of TfR hnRNA assay, no significant changes in the density of nascent TfR mRNA, in comparison to those of GAPDH and S15, were identified between control and manganese-treated groups. Collectively, these studies suggest that manganese exposure did not affect the transcriptional regulation of TfR gene expression.

The mRNAs encoding TfR and ferritin possess one or more unique stem-loop structures common to iron responsive elements (IREs). Binding and unbinding of IRPs to the stem-loops determine the cellular production of TfR and ferritin. The active center of IRP1 possesses an interchangeable cubic structure between [3Fe-4S] and [4Fe-4S] cluster. Under the normal condition, a reductive switch of the [3Fe-4S] cluster to [4Fe-4S] cluster is required for aconitase activity (Beinert and Kennedy, 1993). The conformational change of IRPs may occur in response to variations of cellular iron concentrations, signaling factors, as well as stress mediators (e.g., nitrogen monoxide, cytokines, and hydrogen peroxide) (Rouault and Klausner, 1996). Our previous investigations suggest that manganese, by catalyzing the conversion of the active site of aconitase from a [4Fe-4S] state to a [3Fe-4S] state, inhibits the protein′s catalytic function, while it may facilitate the transformation of the protein to an mRNA binding protein. The latter form promotes its binding to IRE stem loop-carrying mRNA (Chen et al., 2001; Zheng et al., 1998a).

In the current study, a gel shift assay was used to determine the binding activity between cellular IRPs and mRNAs containing the stem-loops. The choroidal epithelial cells treated with manganese displayed a remarkable increase in binding of IRP1 to stem loop mRNAs in comparison to controls. Binding of IRP2, which shares 61% overall amino acid identity with IRP1, but lacks aconitase activity (Guo et al., 1995), to IRE-containing mRNA was also increased by manganese treatment. Our results are in agreement with the studies conducted in PC12 cells by Kwik-Uribe et al. (2003), who reported an 80% increase of binding activity of IRP1 to TfR mRNA following manganese exposure. Thus, the increased cellular levels of TfR mRNA and TfR proteins appear to be due to a post-transcriptional modulation by manganese on protein–mRNA interaction, thereby stimulating the production of TfR. A direct consequence of this protein–mRNA interaction in the neuronal type of cells is the cellular overload of iron with the subsequent iron-initiated oxidative damage. In the blood–CSF barrier, manganese-induced IRPs–mRNA interaction may lead to an enhanced transport of iron at the barrier.

The Transwell model with the primary culture of choroidal epithelial cells has been used to evaluate the *trans*-epithelial transport of materials (Zheng and Zhao, 2002a; Zheng et al., 1999a). Upon formation of an impermeable monolayer at days 7–8, trace amounts of ^{59}Fe were added to the outer (donor) chamber. The rate of appearance of ^{59}Fe radioactivity in the inner (acceptor) chamber thus represents transepithelial transport of ^{59}Fe. Exposure to manganese apparently promoted the transport of ^{59}Fe across the choroidal epithelial barrier. This observation may explain the elevated iron concentration in the CSF following in vivo manganese exposure (Zheng et al., 1999b). More interestingly, there was a vast reduction in ^{59}Fe storage in the choroidal epithelial cells as compared to controls.

Iron is stored in ferritin, which contains 24 subunits, made of heavy (H) and light (L) polypeptide chains that are encoded by different genes, surrounding a cavity in which the iron deposits (Lawson et al., 1991; Munro, 1993). The H-chain is responsible for the rapid oxidation, storage, and uptake of iron (Cozzi et al., 2000) and acts as a regulator of the cellular labile iron pool and an attenuator of the cellular oxidative response (Epsztejn et al., 1999; Geiser et al., 2003), whereas the L-chain creates the nucleation site for iron and formation of the iron core, a complex of iron, phosphate and oxygen (Munro, 1993; Ponka et al., 1998). Our investigation on the ferritin mRNA expression revealed a significant reduction of intracellular ferritin mRNA levels following manganese exposure, especially ferritin heavy chain, implying an altered iron storage and elevated cellular oxidative stress. It is conceivable that binding of IRPs to the IRES in the 5′ UTR of ferritin mRNA may suppress the production of ferritin and decrease cellular iron storage.

In summary, the results in the present study demonstrate that alteration by manganese of cellular TfR takes place at the translational level on IRPs–mRNA interaction, but not at the level of TfR gene transcription. At the blood–CSF barrier, manganese, upon entering the epithelial cells, may replace iron in [Fe-S] cluster of IRP1, which in turn facilitates the binding of IRPs to mRNAs containing stem-loop structure. The up-regulation of TfR along with the down-regulation of ferritin at the blood–CSF barrier thus promotes the influx of iron from systemic circulation to the cerebral compartment.

Acknowledgments

The authors wish to acknowledge the assistance of Dr. Chaoyin Zhang of University of Toronto for designing the primers of TfR hnRNA and TfR RNA. Special appreciation is also extended to Dr. Gregory A. Freyer at Columbia University for designing and providing the template of ferritin-IRE and to Rick Pilsner and Ling Lu for their technical assistance.

This project was partly supported by USA-National Institute of Environmental Health Sciences Grant ES-08146 and PRC-National Natural Science Foundation Grant 30000140.

References

Berg, D., Gerlach, M., Youdim, M.B., Double, K.L., Zecca, L., Riederer, P., Becker, G., 2001. Brain iron pathways and their relevance to Parkinson's disease. J. Neurochem. 79, 225–236.

Beinert, H., Kennedy, M.C., 1993. Aconitase, a two-faced protein: enzyme and iron regulatory factor. FASEB J. 7, 1442–1449.

Burdo, J.R., Connor, J.R., 2001. Iron transport in the central nervous system. In: Templeton, D. (Ed.), Cellular and Molecular Mechanism of Iron Transport. Marcel Dekker Inc., New York, pp. 487–505.

Chen, J.Y., Tsao, G., Zhao, Q., Zheng, W., 2001. Differential cytotoxicity of Mn(II) and Mn(III): special reference to mitochondrial [Fe-S] containing enzymes. Toxicol. Appl. Pharmacol. 175, 160–168.

Connor, J.R., Benkovic, S.A., 1992. Iron regulation in the brain: histochemical, biochemical, and molecular considerations. Ann. Neurol. 32, S51–S61 (Suppl.).

Cozzi, A., Corsi, B., Levi, S., Santambrogio, P., Albertini, A., Arosio, P., 2000. Overexpression of wild type and mutated human ferritin H-chain in HeLa cells: in vivo role of ferritin ferroxidase activity. J. Biol. Chem. 275, 25122–25129.

Danzi, S., Ojamaa, K., Klein, I., 2003. Triiodothyronine-mediated myosin heavy chain gene transcription in the heart. Am. J. Physiol.: Heart Circ. Physiol. 284, H2255–H2262.

David, F.L., Carvalho, M.H., Cobra, A.L., Nigro, D., Fortes, Z.B., Reboucas, N.A., Tostes, R.C., 2001. Ovarian hormones modulate endothelin-1 vascular reactivity and mRNA expression in DOCA-salt hypertensive rats. Hypertension 38, 692–696.

Deane, R., Kong, B., Pilsner, R., Zheng, W., 2002. Brain regional influx of ^{59}Fe: effect of in vivo manganese exposure. Toxicol. Sci. 66 (1-S), 1004 (Supplement).

Deane, R., Zheng, W., Zlokovic, B.V., 2004. Brain capillary endothelium and choroid plexus epithelium regulate transport of transferrin-bound and free iron into the rat brain. J. Neurochem. 88, 813–820.

Delany, A.M., 2001. Measuring transcription of metalloproteinase genes. Methods Mol. Biol. 151, 321–333.

Double, K.L., Gerlach, M., Youdim, M.B., Riederer, P., 2000. Impaired iron homeostasis in Parkinson's disease. J. Neural. Transm., Suppl. 60, 37–58.

Epsztejn, S., Glickstein, H., Picard, V., Slotki, I.N., Breuer, W., Beaumont, C., Cabantchik, Z.I., 1999. H-ferritin subunit overexpression in erythroid cells reduces the oxidative stress response and induces multidrug resistance properties. Blood 94, 3593–3603.

Geiser, D.L., Chavez, C.A., Flores-Munguia, R., Winzerling, J.J., Pham, D.Q., 2003. Aedes aegypti ferritin. Eur. J. Biochem. 270, 3667–3674.

Gerlach, M., Double, K.L., Ben-Shachar, D., Zecca, L., Youdim, M.B., Riederer, P., 2003. Neuromelanin and its interaction with iron as a potential risk factor for dopaminergic neurodegeneration underlying Parkinson's disease. Neurotox. Res. 5, 35–44.

Giometto, B., Bozza, F., Argentiero, V., Gallo, P., Pagni, S., Piccinno, M.G., Tavolato, B., 1990. Transferrin receptors in rat central nervous system. An immunocytochemical study. J. Neurol. Sci. 98, 81–90.

Guo, B., Brown, F.M., Phillips, J.D., Yu, Y., Leibold, E.A., 1995. Characterization and expression of iron regulatory protein 2 (IRP2). Presence of multiple IRP2 transcripts regulated by intracellular iron levels. J. Biol. Chem. 270, 16529–16535.

Jefferies, W.A., Brandon, M.R., Hunt, S.V., Williams, A.F., Gatter, K.C., Mason, D.Y., 1984. Transferrin receptor on endothelium of brain capillaries. Nature 312, 162–163.

Jenner, P., 2003. Oxidative stress in Parkinson's disease. Ann. Neurol. 53 (Suppl. 3), S26–S36 (discussion S36-38).

Johnson, M.D., Anderson, B.D., 1999. In vitro models of blood–brain barrier to polar permeants: comparison of transmonolayer flux measurements and cell uptake kinetics using cultured cerebral capillary endothelial cells. J. Pharm. Sci. 88, 620–625.

Kissel, K., Hamm, S., Schulz, M., Vecchi, A., Garlanda, C., Engelhardt, B., 1998. Immunohistochemical localization of the murine transferrin receptor (TfR) on blood–tissue barriers using a novel anti-TfR monoclonal antibody. Histochem. Cell Biol. 110, 63–72.

Klausner, R.D., Rouault, T.A., Harford, J.B., 1993. Regulating the fate of mRNA: the control of cellular iron metabolism. Cell 72, 19–28.

Kwik-Uribe, C.L., Reaney, S., Zhu, Z., Smith, D., 2003. Alterations in cellular IRP-dependent iron regulation by in vitro manganese exposure in undifferentiated PC12 cells. Brain Res. 973, 1–15.

Lagrange, P., Romero, I.A., Minn, A., Revest, P., 1999. Transendothelial permeability changes induced by free radicals in an in vitro model of the blood–brain barrier. Free Radical Biol. Med. 27, 667–672.

Lawson, D.M., Artymiuk, P.J., Yewdall, S.J., Smith, J.M.A., Livingstone, J.C., Treffry, A., Luzzago, A., Levi, S., Arosio, P., Cesareni, G., Thomas, C.D., Shaw, W.V., Harrison, P.M., 1991. Solving the structure of human H ferritin by genetically engineering intermolecular crystal contacts. Nature 349, 541–544.

Leibold, E.A., Munro, H.N., 1988. Cytoplasmic protein binds in vitro to a highly conserved sequence in the 5′ untranslated region of ferritin heavy- and light-subunit mRNAs. Proc. Natl. Acad. Sci. U.S.A. 85, 2171–2175.

Lin, E., Graziano, J.H., Freyer, G.A., 2001. Regulation of the 75-kDa subunit of mitochondrial complex I by iron. J. Biol. Chem. 276, 27685–27692.

Liu, J., Xie, Y., Ward, J.M., Diwan, B.A., Waalkes, M.P., 2004a. Toxicogenomic analysis of aberrant gene expression in liver tumors and nontumorous livers of adult mice exposed in utero to inorganic arsenic. Toxicol. Sci. 77, 249–257.

Liu, J., Walker, N., Waalkes, M.P., 2004b. Hybridization buffer systems impact the quality of filter array data. J. Pharmacol. Toxicol. Methods 50, 67–71.

Loeffler, D.A., Connor, J.R., Juneau, P.L., Snyder, B.S., Kanaley, L., DeMaggio, A.J., Nguyen, H., Brickman, C.M., LeWitt, P.A., 1995. Transferrin and iron in normal, Alzheimer's disease, and Parkinson's disease brain regions. J. Neurochem. 65, 710–724.

Marton, L.S., Wang, X., Kowalczuk, A., Zhang, Z.D., Windmeyer, E., Macdonald, R.L., 2000. Effects of hemoglobin on heme oxygenase gene expression and viability of cultured smooth muscle cells. Am. J. Physiol.: Heart Circ. Physiol. 279, H2405–H2413.

Mikulits, W., Schranzhofer, M., Beug, H., Mullner, E.W., 1999. Post-transcriptional control via iron-responsive elements: the impact of aberrations in hereditary disease. Mutat. Res. 437, 219–230.

Moos, T., Morgan, E.H., 2000. Transferrin and transferrin receptor function in brain barrier systems. Cell. Mol. Neurobiol. 20, 77–95.

Munro, H., 1993. The ferritin genes: their response to iron status. Nutr. Rev. 51, 65–73.

Pastorcic, M., Das, H.K., 2002. Activation of transcription of the human presenilin 1 gene by 12-*O*-tetradecanoylphorbol 13-acetate. Eur. J. Biochem. 269, 5956–5962.

Ponka, P., Lok, C.N., 1999. The transferrin receptor: role in health and disease. Int. J. Biochem. Cell Biol. 31, 1111–1137.

Ponka, P., Beaumont, C., Richardson, D.R., 1998. Function and regulation of transferrin and ferritin. Semin. Hematol. 35, 35–54.

Rao, D.B., Wong, B.A., McManus, B.E., McElveen, James, A.R., Dorman, D.C., 2003. Inhaled iron, unlike manganese, is not transported to the rat brain via the olfactory pathway. Toxicol. Appl. Pharmacol. 193, 116–126.

Rouault, T.A., Klausner, R.D., 1996. The impact of oxidative stress on eukaryotic iron metabolism. EXS 77, 183–197.

Walker, N.J., 2001. Real-time and quantitative PCR: applications to mechanism-based toxicology. J. Biochem. Mol. Toxicol. 15, 121–127.

Yantiri, F., Andersen, J.K., 1999. The role of iron in Parkinson disease and 1-methyl-4-phenyl-1,2,3,6-tetrahydropyridine toxicity. IUBMB Life 48, 139–141.

Youdim, M.B., 2003. What have we learnt from CDNA microarray gene expression studies about the role of iron in MPTP induced neurodegeneration and Parkinson's disease? J. Neural. Transm., Suppl. 65, 73–88.

Zheng, W., 2001. Toxicology of choroid plexus: special reference to metal-induced neurotoxicities. Micros. Res. Tech. 52, 89–103.

Zheng, W., Zhao, Q., 2001. Iron overload following manganese exposure in cultured neuronal, but not neuroglial cells. Brain Res. 897, 175–179.

Zheng, W., Zhao, Q., 2002a. The blood–CSF barrier in culture: development of a primary culture and transepithelial transport model from choroidal epithelial cells. Methods Mol. Biol. 188, 99–114.

Zheng, W., Zhao, Q., 2002b. Establishment and characterization of an immortalized Z310 choroidal epithelial cell line from murine choroid plexus. Brain Res. 958, 371–380.

Zheng, W., Ren, S., Graziano, J.H., 1998a. Manganese inhibits mitochondrial aconitase: a mechanism of manganese neurotoxicity. Brain Res. 799, 334–342.

Zheng, W., Zhao, Q., Graziano, J.H., 1998b. Primary culture of choroidal epithelial cells: characterization of an in vitro model of blood–CSF barrier. In Vitro Cell Dev. Biol.: Anim. 34, 40–45.

Zheng, W., Blaner, W.S., Zhao, Q., 1999a. Inhibition by lead of production and secretion of transthyretin in the choroid plexus: its relation to thyroxine transport at blood–CSF barrier. Toxicol. Appl. Pharmacol. 155, 24–31.

Zheng, W., Zhao, Q., Slavkovich, V., Aschner, M., Graziano, J.H., 1999b. Alteration of iron homeostasis following chronic exposure to manganese in rats. Brain Res. 833, 125–132.

Zheng, W., Aschner, M., Ghersi-Egea, J.F., 2003. Brain barrier systems: a new frontier in metal neurotoxicological research. Toxicol. Appl. Pharmacol. 192, 1–11.